Investigation of Wear Behavior of Borided DIN X15CrNiSi25 Steel

İsmail Yıldız*
Department of Machine Education, Iscehisar Vocational Schools,
Afyon Kocatepe University, Afyonkarahisar, Turkey

İbrahim Güneş
Department of Metallurgical and Materials Engineering,
Faculty of Technology, Afyon Kocatepe University, Afyonkarahisar, Turkey

*

ABSTRACT

In the present study, effect of the boriding process on adhesion and tribological properties of DIN X15CrNiSi25 steel has been investigated. Boriding was performed in a solid medium consisting of Ekabor-II powders at 1123 and 1323K for 2 and 6 h. The boride layer was characterized by optical microscopy, X-ray diffraction technique and the micro-Vickers hardness tester. . X-ray diffraction analysis of boride layers on the surface of the steels revealed the existence of Fe_xB_y, Cr_xB_y and Ni_xB_y compounds. Depending on the chemical composition of substrates, the boride layer thickness on the surface of the X15CrNiSi25 steel was found to be 56.74 μm. The hardness of the boride compounds formed on the surface of the X15CrNiSi25 steel ranged from 1658 to 2284 $HV_{0,1,}$ whereas Vickers hardness values of the untreated steel X15CrNiSi25 were 276 $HV_{0,1}$. The wear tests were carried out in a ball-disc arrangement under a dry friction condition at room temperature with an applied load of 10N and with a sliding speed of 0.3 m/sec at a sliding distance of 1000m. The wear surfaces of the steel were analyzed using a SEM microscopy and X-ray energy dispersive spectroscopy EDS. It was observed that the wear rate of unborided and borided X15CrNiSi25 steel ranged from 4.57 to 71.42 mm^3/Nm.

Keywords: X15CrNiSi25, Boriding, Micro-Hardness, Tribology

1 INTRODUCTION

Boriding is a thermochemical surface hardening process which occurs with the diffusion of boron atoms on the matrix surface. The introduced boron atoms react with the material and form a number of borides. As a result of these formations, boronizing of materials surface allows to reduce essentially a rate of corrosion, oxidation or shaping of fatigue cracks happening in an outcome of its operation [1]. But the main advantage of boronizing metals is the possibility to alloy a high surface hardness with a low friction coefficient. This leads to a good wear resistance [2]. Because the relationship between the surface hardness and wear rates of the boronized samples also confirms that the wear resistance is improved with the hardness increasing [3,4].

Wear is one of the most common causes of failure in moving components [5]. In general, two approaches have been taken to deal with this, firstly by improving the wear resistance of the parts, and secondly to repair the worn parts after reduction of part thickness [6,7]. In the case of steel components, increasing the hardness through carburizing or nitriding, formation of tempered martensite, cold working and heat treatment, chemical vapor deposition coating and diffusion coating are useful; however, these do not address material loss [8-10]. Thermal spraying is a conventional way to compensate the material loss and to provide desired propertieson parts surfaces; however, the coating processes may introduce porosity or produce weak adhesion in the sprayed coating and deteriorate performance [11,12].

The wear rates can also be related to chemical composition, volume of different microstructural constituents, as well as the matrix structure. Other factors which may also play important role are microstructures and their features [13-15], hardness, work hardening index, fracture and fatigue properties, and stacking fault energy, etc. These do not affect the wear properties in an independent way, but are related to each other in a complex manner. Out of the above, microstructures have a dominant influence on the surface life of machine parts, especially those operating under high sliding velocities and loads [16-18].

Stainless steels have good corrosion resistance due to formation of tightly coherent, adherent, insulating and renewable chromium oxide film on the surface on the order of only a few atom layers in thickness. Therefore, they are used in wide range of goods such as implant material, furniture, automotive trims and cutlery where both aesthetic appearance and corrosion resistance are important design criteria [19,20]. The main objective of this study was to investigate the effect of the boriding process on wear behavior of borided X15CrNiSi255 steel. Structural and wear properties were investigated using optical microscopy, XRD, SEM, EDS, microhardness tests and a ball-on-disc tribotester.

2 MATERIALS AND METHODS

The X15CrNiSi25 stainless steel essentially contained 0.25 wt.% C, 0.85 wt.% Mn, 25.0 wt.% Cr, 19.50 wt.% Ni and 1.50 wt.% Si. The test specimens were cut into Ø25x10mm dimensions, ground up to 1000G and polished using diamond solution. The boriding heat treatment was carried out in a solid medium containing an Ekabor-II powder mixture placed in an electrical resistance furnace operated at the temperature of 1123 and 1323K for 2 and 6 h under atmospheric pressure. Following the completion of the boriding process, test specimens were removed from the sealed in a stainless steel container and allowed to cool down in still air. The microstructures of polished and etched cross-sections of the specimens were observed under a Nikon MA100 optical microscope. The presence of borides formed in the coating layer was confirmed by means of X-ray diffraction equipment (Shimadzu XRD 6000) using Cu Kα radiation. The hardness measurements of the boride layer on steel and untreated steel substrate were made on the cross-sections using a Shimadzu HMV-2 Vickers indenter with a 100 g load.

To perform friction and wear of borided samples a ball-on-disc test device was used. In the wear tests, WC-Co balls of 8 mm in diameter supplied by H.C. Starck Ceramics GmbH were used. Errors caused by the distortion of the surface were eliminated by using a separate abrasion element (WC-Co ball) for each test. The wear experiments were carried out in a ball-disc arrangement under a dry friction condition at room temperature with an applied load of 10N and with sliding speeds of 0.3 m/s at a sliding distance of 1000 m. Before and after each wear test, each sample and abrasion element was cleaned with alcohol. After the test, the wear volumes of the samples were quantified by multiplying the cross-sectional areas of the wear by the width of the wear track obtained from the Taylor-Hobson Rugosimeter Surtronic 25 device. The wear rate was calculated with the following Eqs. (1):

$$\mathrm{Wk} = \frac{Wv}{M\,.S}\, mm^{3} / Nm \qquad (1)$$

Where Wk is the wear rate, Wv the worn volume, M the applied load and S is the sliding distance. Friction coefficients depending on sliding distance were obtained through a friction coefficient program. Surface profiles of the wear tracks on the samples and surface roughness were measured by a Taylor-Hobson Rugosimeter Surtronic 25. Worn surfaces were investigated by scanning electron microscopy (SEM) and energy-dispersive X-ray spectroscopy (EDS).

3. RESULTS AND DISCUSSION

The cross-section of the optical micrographs of the borided X15CrNiSi25 steel at the temperature of 1123K and 1323K for 2 and 6 h are shown in Figure 1. As can be seen the borides formed on the X15CrNiSi25 steel have a smooth and regular morphology. It was found that the coating/matrix interface and matrix could be significantly distinguished and the boride layer had a not columnar structure. . The boride layer hardness of the sample borided at 1323K for 6 h was found to be 56.74 µm, the boride layer hardness of the sample borided at 1323K for 2h was 25.62 µm, the boride layer hardness of the sample borided at 1123K for 6 h was 16.94 µm, while the boride layer hardness of the sample borided at 1123K for 2 h was 7.82 µm.

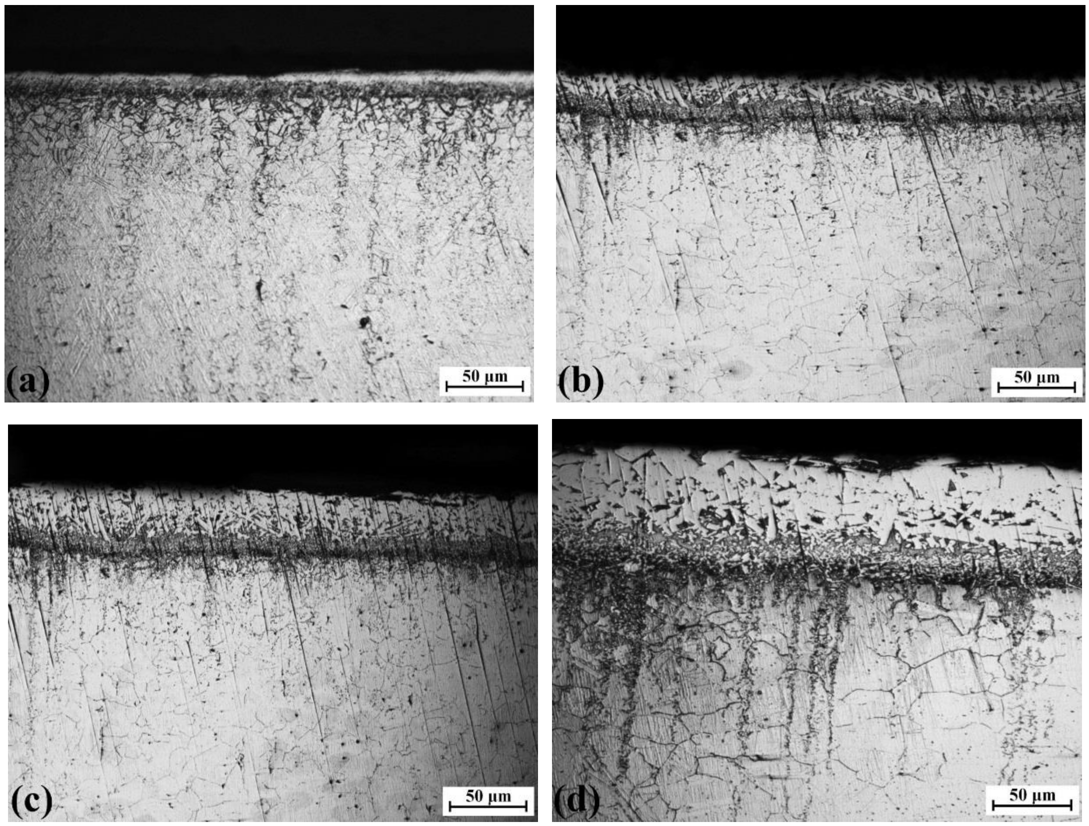

Figure 1: The cross-section of borided X15CrNiSi25 steel; a) 1123K - 2h, b) 1123K - 6h, c) 1323K - 2h, d) 1323K - 6h.

Figure 2 give the XRD pattern obtained at the surface of borided X15CrNiSi25 steel at 1123K and 1323K for treatment time 2 and 6 h.

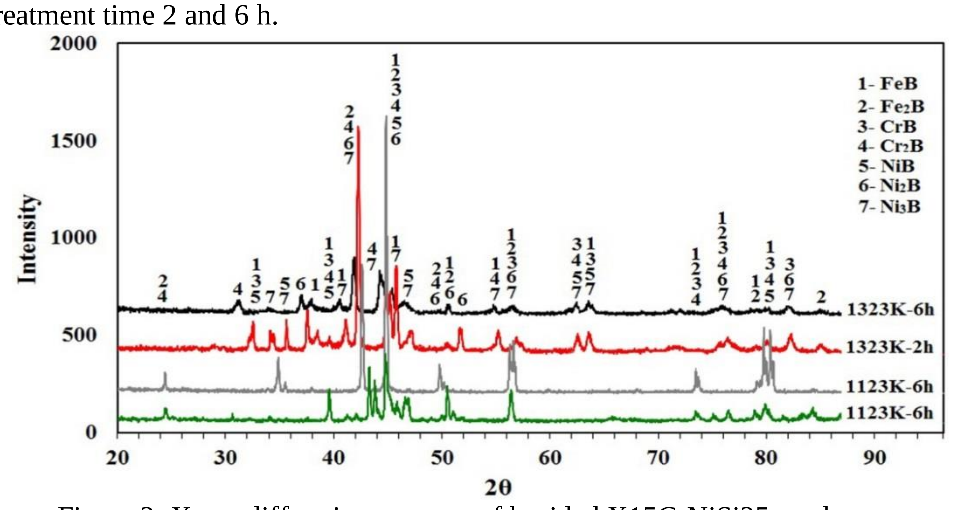

Figure 2: X-ray diffraction patterns of borided X15CrNiSi25 steel

XRD patterns show that the boride layer consists of borides such as MB and M_2B (M=Metal; Fe, Cr, Ni). XRD results showed that boride layers formed on the X15CrNiSi25 stainless steel contained FeB, Fe_2B, CrB, Cr_2B, NiB, Ni_2B, Ni_3B phases. With increasing time and temperature, Fe_2B phase content decreases and FeB, CrB, NiB phase content increases for X15CrNiSi25 steel. The boride layers mainly consist of double intermetallic phase (FeB and Fe_2B) as a result of diffusion of boron atoms from boriding compound to metallic lattice with respect to the holding time.

Micro-hardness measurements were carried out from the surface to the interior along a line in order to see the variations in the boride layer hardness, transition zone and matrix, respectively (Figure 3). Micro-hardness of the boride layers was measured at 10 different locations at the same distance from the surface and the average value was taken as the hardness. The boride layer hardness of the sample borided at 1323K for 6 h was found to be 2284 $HV_{0,1}$, the boride layer hardness of the sample borided at 1323K for 2h was 1972 $HV_{0,1}$, the boride layer hardness of the sample borided at 1123K for 6 h was 1785 $HV_{0,1}$, while the boride layer hardness of the sample borided at 1123K for 2 h was 1658 $HV_{0,1}$. On the other hand, Vickers hardness values were 276 $HV_{0,1}$, for the untreated X15CrNiSi25 steel.

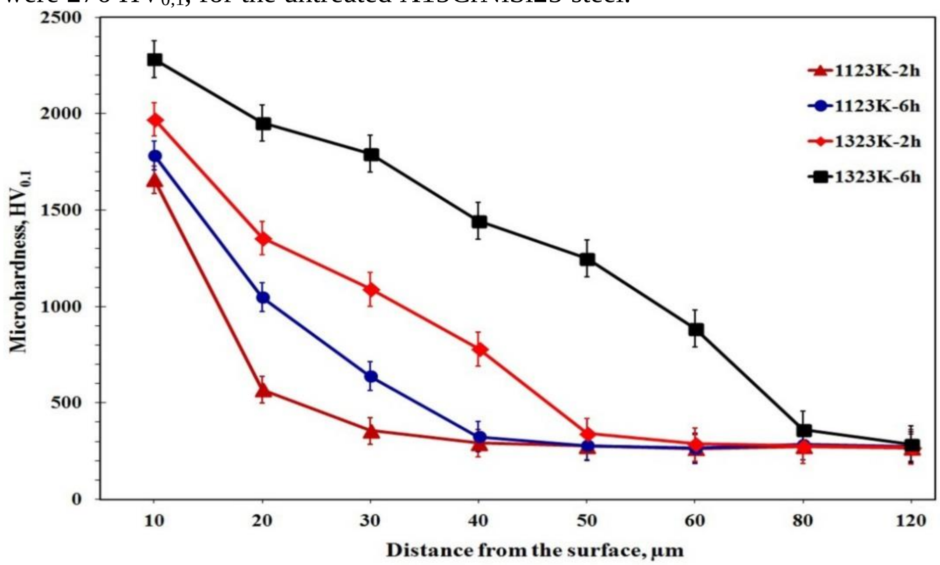

Figure 3: The variation of hardness depth in the borided X15CrNiSi25 steel

Figure 3 show that increasing the boriding temperature and treatment time increases the boride layer hardness. When the hardness of the boride layer is compared with the matrix, boride layer hardness is approximately eight times greater than that of the matrix (1323K for 6 h).

Table 1 shows the surface roughness values of the borided and unborided X15CrNiSi25 steel. The surface roughness of the sample borided at 1123K for 2 h was found to be 0.36 µm, the boride layer hardness of the sample borided at 1123K for 6 h was 0.41 µm, the boride layer hardness of the sample borided at 1323K for 2 h was 0.47 µm, while the boride layer hardness of the sample borided at 1323K for 6 h was 0.54 µm. On the other hand, surface roughness value was 0.11 µm, for the untreated X15CrNiSi25 steel.

Table1 Surface roughness values of the unborided and borided X15CrNiSi25 steel

Unborided	**Borided**			
	1123K - 2 h	**1123K - 6 h**	**1323K - 2 h**	**1323K - 6 h**
0.11	0.36	0.41	0.47	0.54

Table 1 shows that increasing the boriding temperature and treatment time increases the surface roughness values. X15CrNiSi25 steel was observed that surface roughness values increased with the boriding treatment. Gunes [21], Ulker [22], and Sahin [23] solid borided steels and reported that surface roughness values increased with an increase in the boriding temperature. On the other hand, the friction coefficients of the unborided and borided stainless steel varied from 0.35 to 0.67, as can be seen in Table 2. With the boriding treatment, a slight reduction was observed in the friction coefficients of the borided steels.

Table 2 The friction coefficients of the unborided and borided X15CrNiSi25 steel

Unborided	**Borided**			
	1123K - 2 h	**1123K - 6 h**	**1223K - 2 h**	**1223K - 6 h**
0.67	0.35	0.44	0.46	0.53

Figure 4 shows the wear rate of the unborided and borided X15CrNiSi25 steel. Reductions in the wear rates of the borided steels were observed according to the unborided steels. Due to the hardness of the FeB and CrB phases, the steel showed more resistance to wear. The lowest wear rate was obtained in the X15CrNiSi25 steel borided at 1323K for 6 hours while the highest wear rate was obtained in the unborided X15CrNiSi25 steel. The wear test results indicated that the wear resistance of borided steels increased considerably with the boriding treatment and time. It is well known that hardness of the boride layer plays an important role in the improvement of wear resistance. As shown in Fig. 3 and Fig. 4, the relationship between the surface microhardness and the wear resistance of the borided samples also confirms that the wear resistance was improved with the hardness increasing. This is in agreement with reports of previous studies [21-24]. When the wear rate of the borided steel is compared with the unborided steel, the wear rate of the borided steels is approximately four times lower than that of the unborided steels.

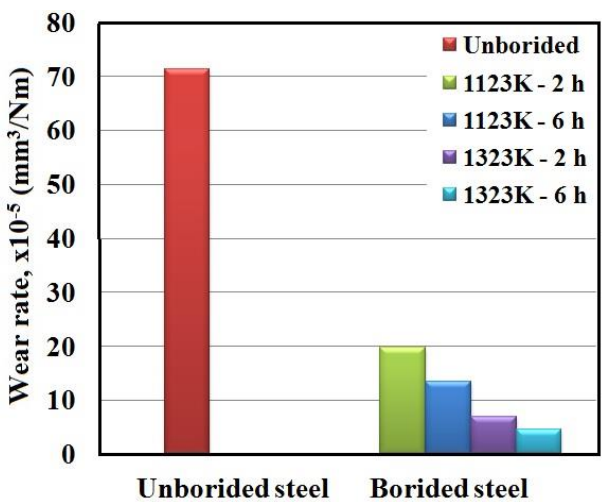

Figure 4: The wear rate of unborided and borided X15CrNiSi25 steel.

The SEM micrographs of the worn surfaces of the unborided and borided X15CrNiSi25 steel are illustrated in Figs. 5 and 6. Figure 5a shows the SEM micrographs of the wear surfaces of the unborided X15CrNiSi25 steel. In Fig. 5a, the worn surface of the unborided steel was rougher and coarser wear debris particles were present. The wear region of the borided steel, debris, delamination wear, surface grooves and cracks on the surface can be observed (Fig. 6). There were micro-cracks, abrasive particles and small holes on the worn surface of the boride coatings. In the wear region of borided X15CrNiSi25 steel, there were cavities probably formed as a result of layer fatigue (Fig. 6) and cracks concluded in delaminating wear. Figure 6 show the wear surfaces, and the cross-sectional surface (CS) of the wear mark obtained from the wear region by analyzing multiple profilometry surface line scans using a Nanovea ST-400 non-contact optical profiler. It was observed that the depth and width of the wear trace on the surfaces of the samples decreased with an increase in the boriding temperature and time (Fig. 6b, 6d, 6f, 6h). Figure 6ı shows the EDS analysis obtained from Figure 6g. Fe-based oxide layers formed as a result of the wear test. The spallation of the oxide layers in the sliding direction and their orientation extending along the wear track were identified. When the SEM image of the worn surfaces of the unborided sample is examined, it can be seen that the wear marks in Fig. 5b is larger and deeper.

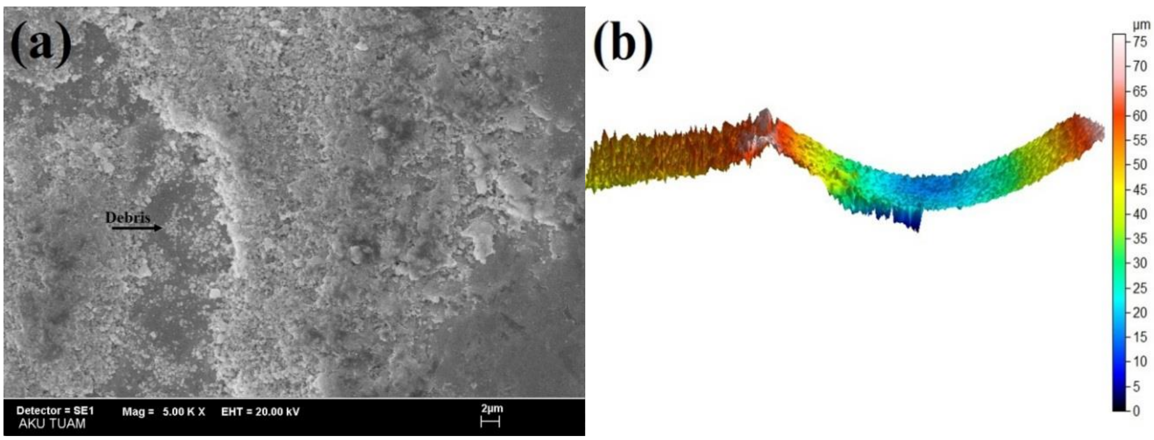

Figure 5: The SEM micrograph and cross-sectional surface of the worn-out surfaces of the unborided X15CrNiSi25 steel; a) unborided, b) cross-sectional surface (CS)

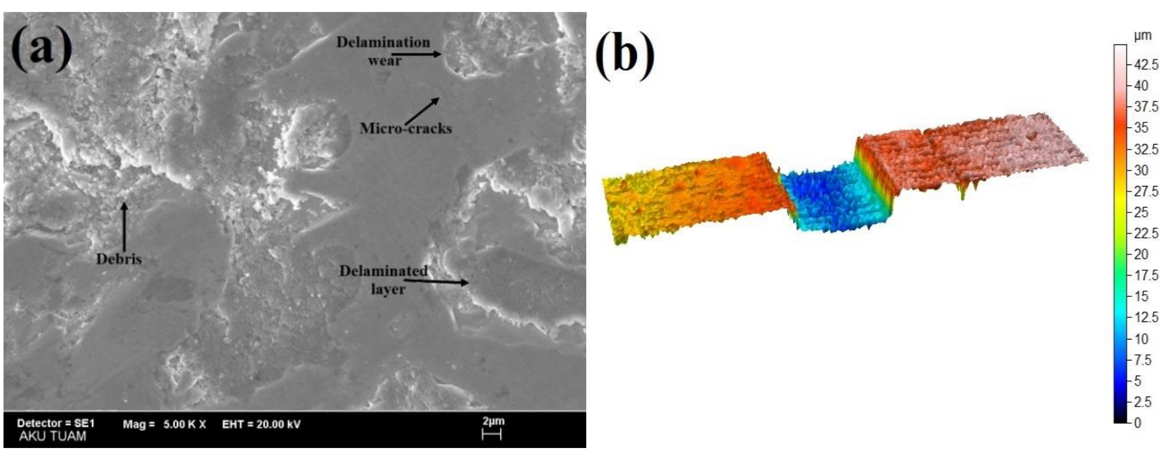

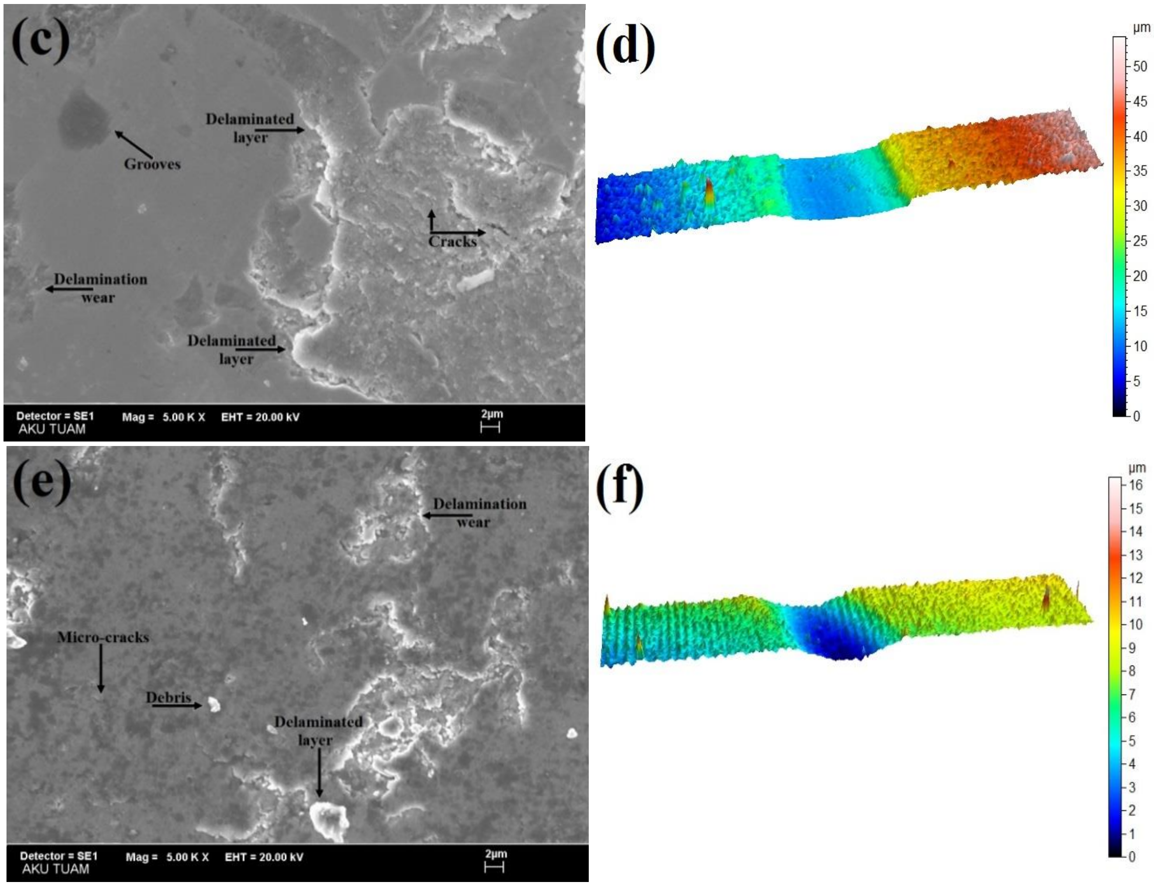

Figure 6: The SEM micrographs and cross-sectional surface of the worn-out surfaces of the borided X15CrNiSi25 steel; a) 1123K – 2 h, b) 1123K – 2 h CS, c) 1123K – 6 h, d) 1123K – 6 h CS, e) 1323K – 2 h, f) 1323K – 2 h CS, g) 1323K – 6 h, h) 1323K – 6 h CS, ı) EDS analysis.

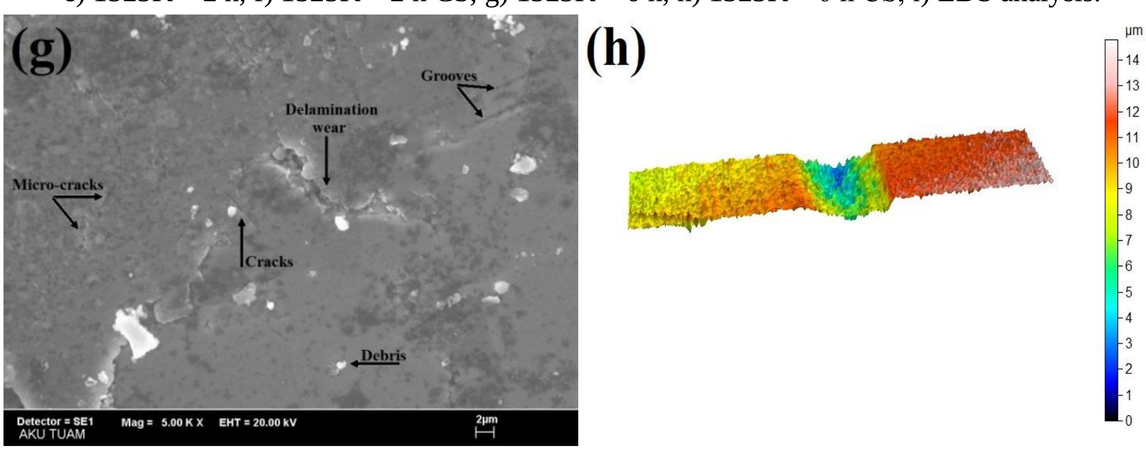

Figure 6 (continue): The SEM micrographs and cross-sectional surface of the worn-out surfaces of the borided X15CrNiSi25 steel; a) 1123K – 2 h, b) 1123K – 2 h CS, c) 1123K – 6 h, d) 1123K – 6 h CS, e) 1323K – 2 h, f) 1323K – 2 h CS, g) 1323K – 6 h, h) 1323K – 6 h CS, ı) EDS analysis.

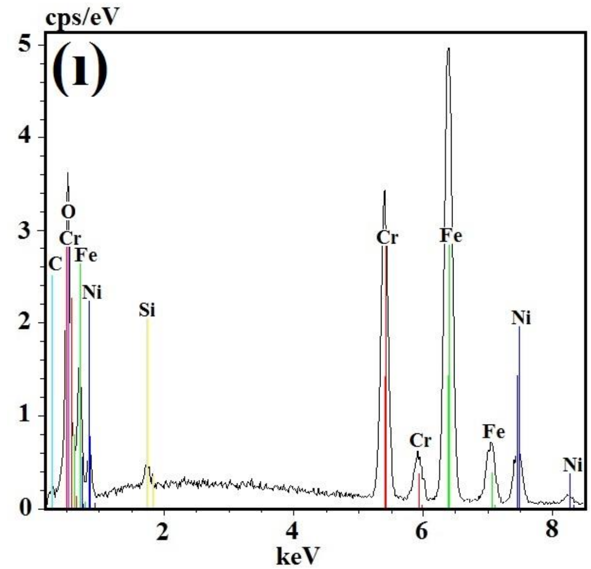

Figure 6 (continue): The SEM micrographs and cross-sectional surface of the worn-out surfaces of the borided X15CrNiSi25 steel; a) 1123K – 2 h, b) 1123K – 2 h CS, c) 1123K – 6 h, d) 1123K – 6 h CS, e) 1323K – 2 h, f) 1323K – 2 h CS, g) 1323K – 6 h, h) 1323K – 6 h CS, ı) EDS analysis.

5. CONCLUSIONS

In this study, wear behavior and some of the mechanical properties of borides on the surface of borided X15CrNiSi25 stainless steel were investigated. Some of the conclusions can be drawn as follows.

- Boride types formed on the surface of the steel have a smooth morphology.
- The boride layer thickness on the surface of the X15CrNiSi25 steel was obtained, depending on the boriding time and temperature, 7.82-56.74 μm.
- The multiphase boride coatings that were thermo chemically grown on the X15CrNiSi25 steel was constituted by the FeB, Fe_2B, CrB, Cr_2B, NiB, Ni_2B and Ni_3B phases.
- The surface hardness of the borided steel was in the range of 1658-2284 $HV_{0,1}$, while for the untreated the steel substrate it was 276 $HV_{0,1}$.
- The lowest wear rate was obtained in the steel borided at 1323K for 6 hours while the highest wear rate was obtained in the unborided steel.
- The wear rate of the borided steel was found to be approximately seven times lower the wear rate of the unborided steel.

REFERENCES

[1] Aytekin, H. and Akcin, Y. (2013). Characterization of borided Incoloy 825 alloy, Materials and Design, 50, 515-521.

[2] Sista, V., Kahvecioglu, O., Kartal, G., Zeng, Q.Z., Kim, J.H., Eryilmaz, O.L. and Erdemir, A. (2013). Evaluation of electrochemical boriding of Inconel 600, Surface & Coatings Technology, 215, 452-459.

[3] Gunes¸ I. and Kayali., Y. (2014). Investigation of mechanical properties of borided Nickel 201 alloy, Materials and Design, 53,577-580.

[4] Cimenoglu, H., Atar, E. and Motallebzadeh, A. (2014). High temperature tribological behaviour of borided surfaces based on the phase structure of the boride layer, Wear, 309,152-158.

[5] Tabura, M., Izciler, M., Gul, F. and Karacan, I. (2009). Abrasive wear behavior of boronized AISI 8620 steel, Wear, 266, 1106-1112.

[6] Ozbek, I. and Bindal, C. (2002). Mechanical properties of boronized AISI W4 steel, Surface and Coatings Technology, 154,14-20.

[7] Ojala, N., Valtonen, K., Heino, V., Kallio, M., Aaltonen, J., Siitonen, P. and Kuokkala, V. T. (2014). Effects of composition and microstructure on the abrasive wear performance of quenched wear resistant steels, Wear, 317, 225-232.

[8] Taktak, S. (2007). Some mechanical properties of borided AISI H13 and 304 steels, Materials and Design, 28, 1836-1843.

[9] Efremenko, V.G., Shimizu, K., Noguchi, T., Efremenko, A.V. and Chabak, Y. G. (2013). Impact abrasive–corrosion wear of Fe-based alloys: Influence of microstructure and chemical composition upon wear resistance, Wear, 305, 155-165.

[10] Mu, D., Shen, B. L. and Zhao, X. (2010). Effects of boronizing on mechanical and dry-sliding wear properties of CoCrMo alloy, Materials and Design, 31, 3933-3936.

[11] Ceschini, L., Chiavari, C., Lanzoni, E. and Martini, C. (2012). Low-temperature carburised AISI 316L austenitic stainless steel: Wear and corrosion behaviour, Materials and Design, 38, 154-160.

[12] Ozkan G. H. (2007). Dry sliding wear in injection molded 17-4 PH stainless powder with nickel boride additions, Wear, 262, 491-497.

[13] Bejar, M. A. and Moreno, E. (2006). Abrasive wear resistance of boronized carbon and low-alloy steels, Journal of Materials Processing Technology, 173, 352-358.

[14] Gunes, I. (2013). Wear Behaviour of Plasma Paste Boronized of AISI 8620 Steel with Borax and B_2O_3 Paste Mixtures, J. Mater. Sci. Technol., 29(7), 662-668.

[15] Rai, D., Singh, B. and Singh, J. (2007). Characterisation of wear behaviour of different microstructures in Ni–Cr–Mo–V steel, Wear, 263, 821-829.

[16] Hardell, J., Kassfeldt, E. and Prakash, B. (2008). Friction and wear behaviour of high strength boron steel at elevated temperatures of up to 800 °C, Wear, 264, 788-799.

[17] Rai, D., Singh, B. and Singh,J. (2007). Characterisation of wear behaviour of different microstructures in Ni–Cr–Mo–V steel, Wear, 263, 821-829.

[18] Hardell, J., Kassfeldt, E., Prakash, B. (2008). Friction and wear behaviour of high strength boron steel at elevated temperatures of up to 800 °C, Wear, 264, 788-799.

[19] Ozdemir, O., Omar, M. A., Usta, M., Zeytin, S., Bindal, C. and Ucısık, A.H. (2009). An investigation on boriding kinetics of AISI 316 stainless steel, Vacuum, 83, 175-179.

[20] Ozbek, I., Konduk, B. A., Bindal, C. and Ucısık, A. H. (2002). Characterization of borided AISI 316L stainless steel implant, Vacuum, 65, 521-525.

[21] Gunes, I. (2014). Tribological Properties and Characterisation of Plasma Paste Borided AISI 5120 Steel, Journal of the Balkan Tribological Association, 20, 351.

[22] Ulker, S., Gunes, I., Taktak, S. (2011). Investigation of tribological behaviour of plasma paste boronized of AISI 8620, 52100 and 440C steels, Indian Journal of Engineering & Materials Sciences, 18, 370-376.

[23] Sahin, S. (2009). Effects of boronizing process on the surface roughness and dimensions of AISI 1020, AISI 1040 and AISI 2714, J. Mater. Process. Tech., 209, 1736–1741.

[24] Mu, D., Shen, B., Zhao, X. (2010). Effects of boronizing on mechanical and dry-sliding wear properties of CoCrMo alloy, Materials and Design, 31, 3933–3936.